ACS OMEGA

Article

Cite This: ACS Omega 2019, 4, 5209−5220

http://pubs.acs.org/journal/acsodf

Computational Study of the Ni-Catalyzed C−H Oxidative Cycloaddition of Aromatic Amides with Alkynes

Humair M. Omer[†] and Peng Liu*[,†,‡]

[†]Department of Chemistry, University of Pittsburgh, Pittsburgh, Pennsylvania 15260, United States

[‡]Department of Chemical and Petroleum Engineering, University of Pittsburgh, Pittsburgh, Pennsylvania 15261, United States

Supporting Information

ABSTRACT: The mechanism of Ni-catalyzed *ortho* C(sp^2)−H oxidative cycloaddition of aromatic amides with internal alkynes containing 2-pyridinylmethylamine directing group was investigated using density functional theory (DFT) calculations. The C−H cleavage step proceeds via σ-complex-assisted metathesis (σ-CAM) with an alkenyl-Ni(II) complex. This is in contrast to the more common carboxylate/carbonate-assisted concerted metalation−deprotonation mechanism in related Ni-catalyzed C−H bond functionalization reactions with *N*,*N*-bidentate directing groups. In this reaction, the alkyne not only serves as the coupling partner, but also facilitates the σ-CAM C−H metalation both kinetically and thermodynamically. The subsequent functionalization of the five-membered nickelacycle proceeds via alkyne insertion into the Ni−C bond to form a seven-membered nickelacycle. This process proceeds with high levels of regioselectivity to form a C−C bond with sterically more encumbered alkyne terminus. This unusual regioselectivity is due to steric repulsions with the directing group that is coplanar with the alkyne in the migratory insertion transition state. The C−N bond reductive elimination to form the isoquinolone cycloadduct is promoted by PPh_3 complexation to the Ni center and the use of flexible 2-pyridinylmethylamine directing group. The origin of the cis−trans isomerism of alkene byproduct was also explained by computations.

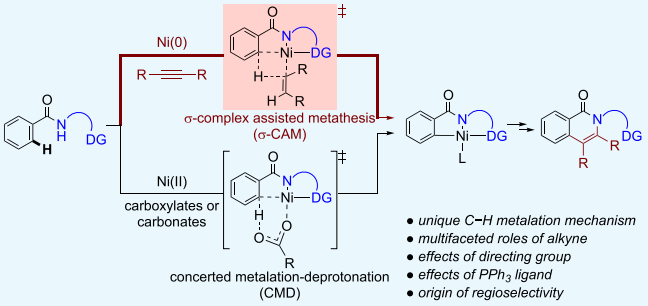

1. INTRODUCTION

Functionalization of C−H bonds to construct new C−C and C−heteroatom bonds using transition-metal catalysts is a powerful, step- and atom-economical strategy in organic synthesis.[1] First introduced by Daugulis et al.,[2] *N*,*N*-bidentate directing groups are now widely used to facilitate site-selective C−H bond functionalizations using a variety of transition metals, including Pd, Ni, Ru, Rh, Co, and Cu, as catalysts (Scheme 1).[3,4] The C−H cleavage step in these reactions is most commonly proposed to proceed via a base-promoted concerted metalation−deprotonation (CMD) mechanism.[5] Although other C−H bond metalation pathways, such as oxidative addition (OA),[6] σ-complex-assisted metathesis (σ-CAM),[7] and ligand-to-ligand hydrogen transfer,[8] are well precedented in the literature, these alternative mechanisms have not been thoroughly investigated in C−H functionalization reactions involving *N*,*N*-bidentate directing groups.[9] Because previous computational mechanistic studies of this type of reactions all focused on the CMD mechanism,[10,11] it is not clear what conditions would promote an alternative C−H bond cleavage pathway. In addition, factors that control the reactivity of these alternative C−H cleavage pathways have not been investigated computationally.

In this manuscript, we report a computational study of the Ni-catalyzed oxidative cycloaddition of aromatic amides and alkynes via C(sp^2)−H functionalization assisted by a 2-pyridinylmethylamine directing group (Scheme 2a).[12,13] In contrast to the C−H functionalization of similar aromatic and aliphatic amides with other coupling partners,[14−18] this oxidative cycloaddition is mechanistically distinct in several aspects. First, unlike the majority of Ni-catalyzed C−H functionalization reactions, which often employs a Ni(II) precatalyst and under conditions with bases (e.g., acetates, carbonates, etc.), this reaction involves a Ni(0) catalyst in the absence of a base. Chatani et al. proposed a unique C−H metalation mechanism via an alkenyl-Ni(II) complex formed from insertion of an alkyne to a nickel(II)-hydride.[12,19] It is surmised that the electron-deficient Ni(II) center would coordinate to the *ortho* C−H bond to form a σ-complex, which then undergoes σ-complex-assisted metathesis (σ-CAM) of the *ortho* C−H bond with the Ni−alkenyl bond via a four-membered cyclic transition state (path b, Scheme 1). Second, this oxidative cycloaddition forms the isoquinolone cycloadduct, while reactions of similar substrates with alkynes under different reaction conditions (e.g., in the presence of a base or with O_2 as oxidant) lead to acyclic alkenylation or alkynation products (Scheme 2b,c).[20] These reactions are expected to involve similar Ni(II) metalacycle intermediates regardless of

Received: January 4, 2019
Accepted: February 1, 2019
Published: March 13, 2019

DOI: 10.1021/acsomega.9b00030
ACS Omega 2019, 4, 5209−5220

Scheme 1. Mechanisms of Transition-Metal-Catalyzed C−H Functionalization of Amides Using *N,N*-Bidentate Directing Groups

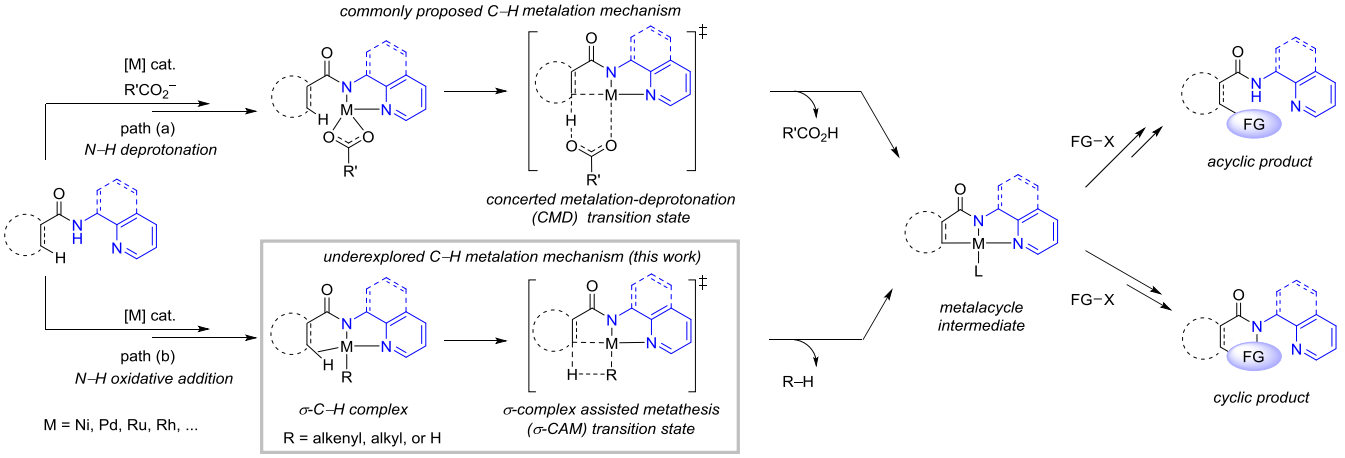

Scheme 2. Ni-Catalyzed C−H Functionalization of Amides with Alkynes Using *N,N*-Bidentate Directing Groups

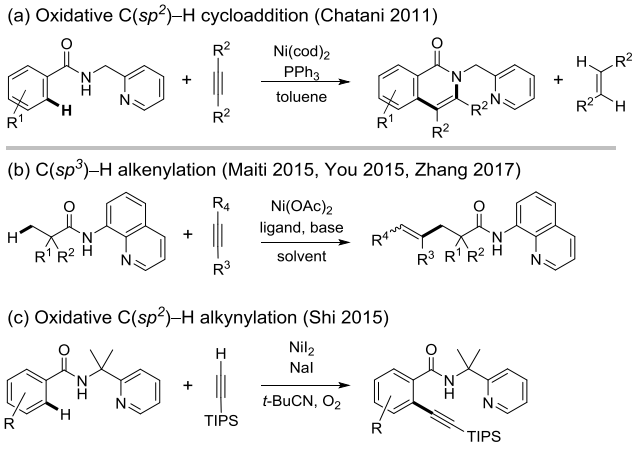

the C−H metalation mechanism (Scheme 1). Factors that determine the chemoselectivity of cyclic versus acyclic products are still not clear. Finally, this oxidative cycloaddition uses alkyne as a mild oxidant,[9,21] which is unusual in oxidative C−H functionalization reactions. In most of the oxidative C−H functionalization reactions,[22−25] the oxidant is not directly involved in the C−H metalation step. In contrast, it has been proposed that the alkyne promotes the reactivity of the C−H metalation step of this reaction.[12] Therefore, the role of the alkyne oxidant warrants an in-depth investigation.

To address these mechanistic ambiguities, we performed density functional theory calculations to investigate the reaction mechanisms of the Ni-catalyzed *ortho* C(sp^2)−H oxidative cycloaddition reaction with alkynes. We provide a detailed analysis of the mechanisms of the C−H metalation step and the role of alkyne in facilitating the C−H metalation. The effects of phosphine additives and 2-pyridinylmethylamine directing group on reactivity and chemoselectivity for the isoquinolone cycloaddition products are carefully analyzed. In addition, the origins of the experimentally observed regioselectivity with unsymmetrically internal aryl alkynes and the formation of *trans*-alkene byproducts are also rationalized.

2. RESULTS AND DISCUSSION

2.1. Proposed Reaction Mechanisms. The proposed mechanisms of the Ni-catalyzed *ortho* C(sp^2)−H oxidative cycloaddition of aromatic amide **1** with model substrate 2-butyne **2** to afford the isoquinolone cycloaddition product **3** are provided in Scheme 3. With the low-valence Ni(0) precatalyst, coordination of the *N,N*-bidentate directing group most likely occurs via an oxidative addition of the amide N−H bond to form a Ni(II)-hydride (**10**) rather than through a base-promoted N−H deprotonation.[26,27] The *ortho* C−H bond in **10** is expected to yield an agostic interaction with the Ni due to its proximity to the electron-deficient metal center. From **10**, two different C−H metalation pathways are possible. The σ-complex-assisted metathesis (σ-CAM) of the *ortho* C−H bond with the Ni−H bond in **10** will afford the H_2-bound nickelacycle **11**.[28] Alternatively, alkyne insertion into the Ni−H bond in **10** will form an alkenyl-Ni(II) complex **8**,[29] which then undergoes a σ-CAM with the Ni−alkenyl bond to give the alkene-bound nickelacycle **9**. Ligand exchange of the H_2 or alkene in intermediate **11** or **9** with an alkyne yields complex **13**. Subsequent alkyne migratory insertion into the Ni−C(sp^2) bond in **13** forms a seven-membered nickelacycle, which upon C−N bond reductive elimination gives the isoquinolone product **3** and regenerates the Ni(0) catalyst. As discussed in Introduction, because such σ-CAM pathways have not been investigated computationally, a few important mechanistic questions still remain. These include: (a) the preference of the two competing σ-CAM pathways from either the nickel hydride **10** or the alkenyl nickel complex **8**; (b) factors that promote the C−N bond reductive elimination to form the cycloaddition product; (c) factors that promote alkyne insertion into the nickelacycle **13** over the direct alkene migratory insertion from **9**; (d) origins of regioselectivity with unsymmetrical internal alkynes; and (e) the mechanism to form the *trans*-alkene byproduct. These questions are discussed in detail in the following sections.

2.2. Mechanisms of the *Ortho* C(sp^2)−H Metalation Step and the Role of Alkyne as a Hydrogen Acceptor. The computed reaction energy profiles for steps leading to the C−H metalated nickelacycle **9** are shown in Figure 1a. Optimized geometries of select transition states and intermediates are shown in Figure 1b. The catalytic cycle begins with ligand exchange to replace the cod ligands in the Ni(cod)$_2$

DOI: 10.1021/acsomega.9b00030
ACS Omega 2019, 4, 5209−5220

Scheme 3. Proposed Mechanisms of the Ni-Catalyzed *Ortho* C(sp^2)−H Oxidative Cycloaddition Reaction

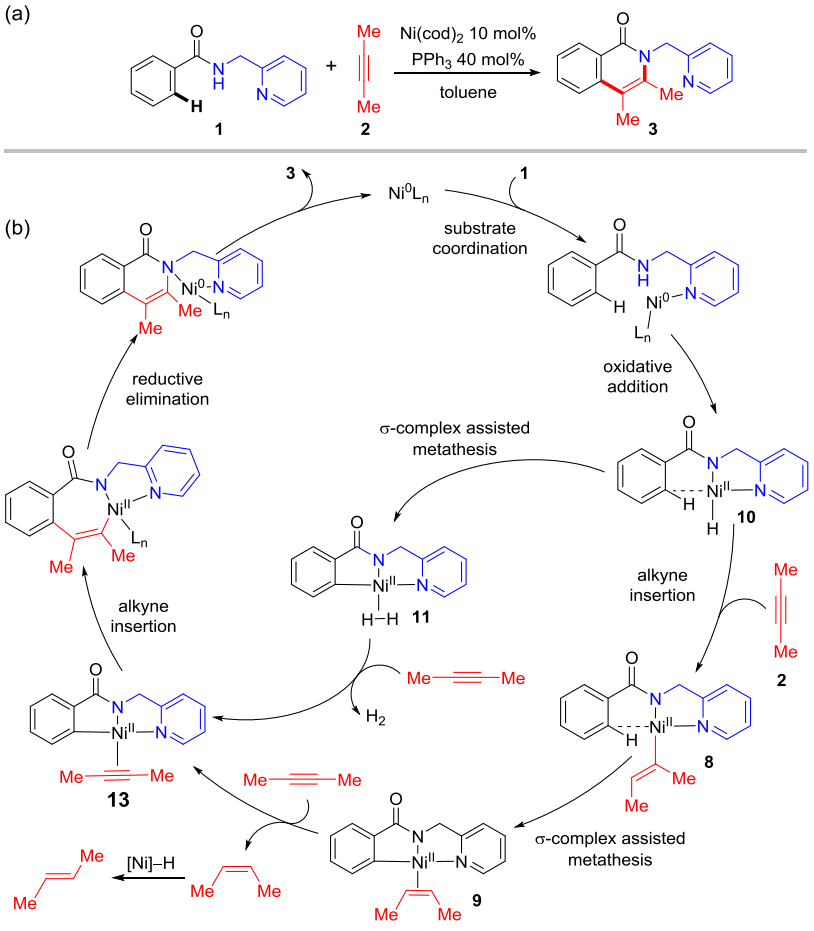

precatalyst with PPh_3 and amide **1** to form complex **4**. Under the experimental conditions of 10 mol % $Ni(cod)_2$, 40 mol % PPh_3 ligand, and three or more equivalents of internal alkyne, cod, PPh_3, or the internal alkyne can potentially bind to the Ni center prior to the amide N−H oxidative addition.[30] The N−H oxidative addition pathways involving these ancillary ligands were considered computationally (see the Supporting Information for details). Our calculations indicate that the most favorable amide N−H oxidative addition pathway involves binding of two PPh_3 ligands (**TS1**). Facilitated by the strong donor ligands (PPh_3 and pyridine), this N−H oxidative addition process has an activation barrier of 28.0 kcal/mol with respect to **1** and $Ni(cod)_2$. In the absence of PPh_3, the N−H oxidative addition requires a barrier that is about 5 kcal/mol higher than that of **TS1** (see the Supporting Information for details).

From the Ni(II)-hydride intermediate **5**, two different σ-CAM pathways are possible. Dissociation of the PPh_3 ligand forms σ-complex **10**, which has a strong agostic interaction between the *ortho* C−H bond and the Ni.[31] This agostic interaction slightly elongates the *ortho* C−H bond to 1.11 Å compared to 1.09 Å for the same bond in **5**. Formation of the σ-complex promotes the σ-bond metathesis of the *ortho* C−H bond with the Ni−H bond via a four-membered cyclic σ-CAM transition state **TS4**.[32] The four-membered cycle in **TS4** is completely planar, which makes the benzene ring coplanar with the 2-pyridinylmethylamine directing group, resembling the planar geometry of the forming nickelacycle intermediate **11**. **TS4** is only 9.2 kcal/mol higher in energy than the σ-complex **10**. However, because the formation of the Ni(II)-hydride σ-complex **10** is highly endergonic (27.1 kcal/mol with respect to amide **1** and the $Ni(cod)_2$ catalyst), the overall activation free energy of this σ-CAM pathway is relatively high ($\Delta G^{\ddagger}$ = 36.3 kcal/mol). An alternative σ-CAM pathway from complex **5** involves a ligand exchange to replace the PPh_3 ligand with an alkyne to form π-alkyne complex **6**, which then undergoes facile alkyne migratory insertion (**TS2**) into the Ni−H bond and forms alkenyl-Ni(II) complex **8**.[33] An agostic interaction with the *ortho* C−H bond was also observed in σ-complex **8**, although the distance between the C−H bond and the Ni is slightly longer than that in **10** due to the larger size of the alkenyl group compared to the hydride ligand. From **8**, the C−H metalation occurs via σ-CAM transition state **TS3**, which requires a low activation barrier of 10.8 kcal/mol with respect to **8** to form the alkene-bound five-membered nickelacycle **9**.[34] Similar to the planar geometry of **TS4**, the four-membered cycle in **TS3** is also coplanar with the bidentate directing group. The alkenyl group is perpendicular to the plane. Therefore, no significant steric repulsions are observed between the alkenyl group and the directing group in the σ-CAM transition state. Overall, **TS3** is much more stable than **TS4** because of the greater stability of the alkenyl-Ni(II) complex **8** compared to the Ni(II)-hydride **10**. As such, the σ-CAM occurs via the alkenyl-Ni(II) complex **8** rather than from the Ni(II)-hydride **10**, consistent with the mechanism proposed by Chatani.[12] Here, the alkyne plays an important role in promoting the C−H metalation via σ-CAM. Although the initial N−H oxidative addition to form the Ni(II)-hydride

DOI: 10.1021/acsomega.9b00030
ACS Omega 2019, 4, 5209−5220

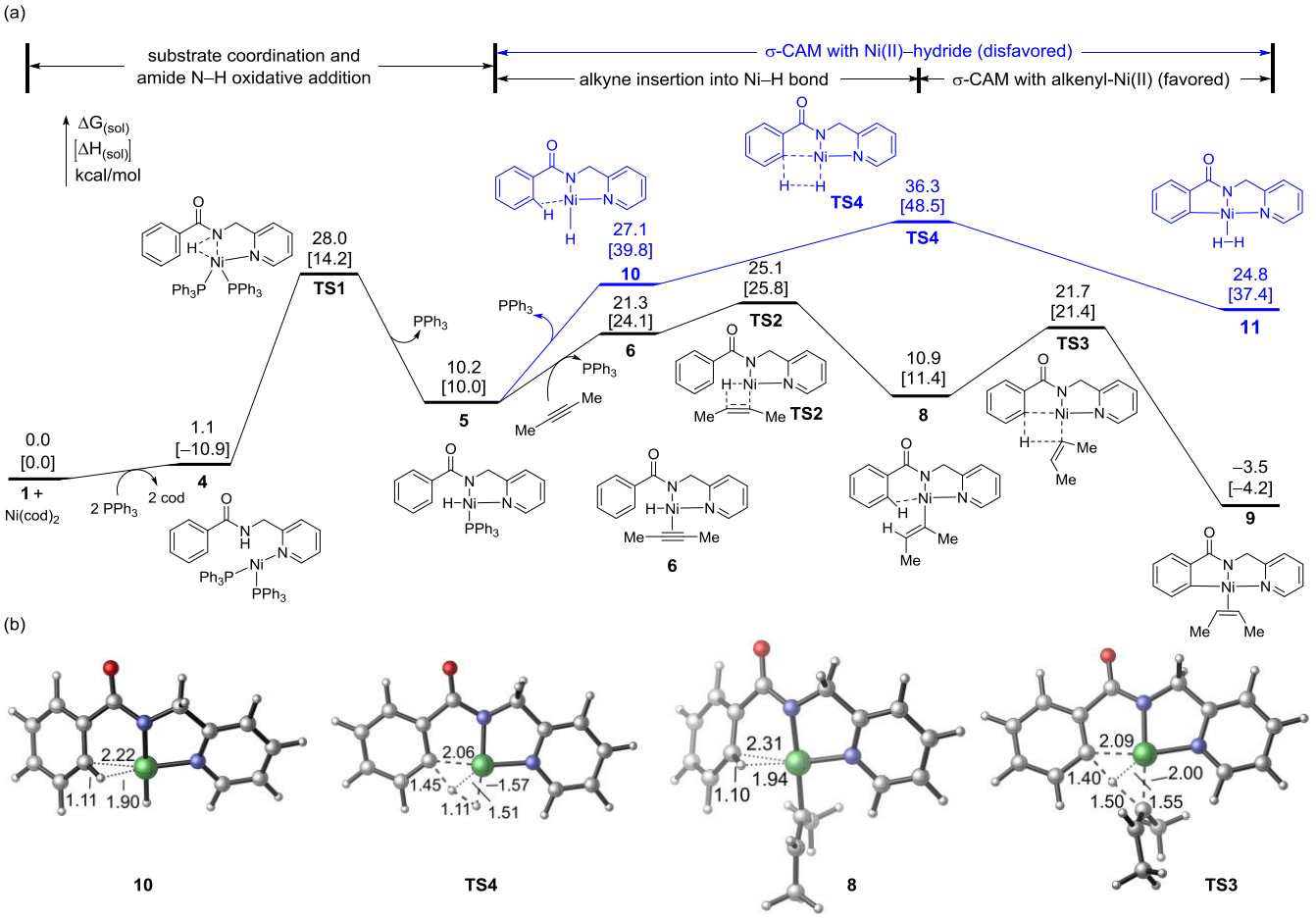

Figure 1. Mechanisms of the C−H metalation steps in the reaction of amide 1 with 2-butyne. (a) Computed reaction energy profiles of Ni-catalyzed *ortho* C(sp^2)−H metalation. (b) Optimized structures of σ-C−H complexes and σ-CAM transition states with select bond distances shown in Å. All energies are with respect to the separate reactants and Ni(cod)$_2$.

is kinetically feasible, this process is thermodynamically uphill. In the presence of alkyne, the Ni(II)-hydride intermediate is converted to a thermodynamically more stable alkenyl-Ni(II) complex via alkyne migratory insertion. Due to the thermodynamic stability of the alkenyl-Ni(II) complex, this σ-CAM pathway now requires a much lower overall activation barrier. As the H_2 acceptor, the alkyne also provides thermodynamic driving force for the C−H metalation. While the formation of the *cis*-2-butene-bound nickelacycle **9** is exergonic, the corresponding C−H metalation process in the absence of alkyne to form the H_2-bound nickelacycle **11** is endergonic by 24.8 kcal/mol with respect to the reactants (**1**, alkyne, and Ni(cod)$_2$). Taken together, the alkyne serves multiple roles in promoting the C−H metalation both kinetically and thermodynamically.[35]

2.3. Mechanisms of Ni−C Insertion and C−N Bond Formation Steps and the Effects of Phosphine Additives and the 2-Pyridinylmethylamine Directing Group. We next investigated the mechanisms of the reaction of the nickelacycle intermediate **9** with alkyne to form the experimentally observed isoquinolone product and a few competing pathways to the experimentally unobserved products (Figure 2). From the alkene-bound nickelacycle **9**, ligand exchange with another molecule of alkyne forms π-alkyne complex **13**, which is 7.8 kcal/mol more stable than **9**. The alkyne migratory insertion to the Ni−C bond in **13** forms a seven-membered nickelacycle **14** via transition state **TS5**. This process is more favorable than the alkene migratory insertion from **9** (via **TS8**). Here, **TS5** is stabilized by the backdonation of the Ni d electrons to the π^* of the alkyne, which is not present in **TS8**.[36] From **14**, the C−N bond reductive elimination is promoted by coordination of a PPh_3 ligand to form a four-coordinated Ni(II) complex **15**. From **15**, the C−N bond reductive elimination (**TS6**) requires only 13.7 kcal/mol to form the isoquinolone-bound Ni(0) complex **16**. On the other hand, reductive elimination from complex **14** without phosphine coordination requires a much higher activation barrier of 24.2 kcal/mol (**TS7**) with respect to **14**.

Experimentally, the Ni-catalyzed *ortho* C(sp^2)−H oxidative cycloaddition reaction is the most effective with 2-pyridinylmethylamine directing group.[12] Although several different *N*,*N*-bidentate directing groups, such as 2-pyridinylmethylamine, 8-aminoquinoline, and 2-(pyridin-2-yl)isopropyl amine, have been used experimentally for related transformations, a thorough understanding of potential directing group effects in these reactions is still lacking.[10a,b] We surmised that the flexible directing group in **1** may facilitate the C−N bond reductive elimination to form the cyclic isoquinolone product. We performed calculations with model substrate **19** containing a more rigid 8-aminoquinoline moiety to explore the flexibility effect of the directing group. In reaction with **19**, the C−N bond reductive elimination (**TS9**) requires an activation barrier of 18.9 kcal/mol with respect to the seven-membered nickelacycle **20** (Figure 3), which is more than 6 kcal/mol

DOI: 10.1021/acsomega.9b00030
ACS Omega 2019, 4, 5209−5220

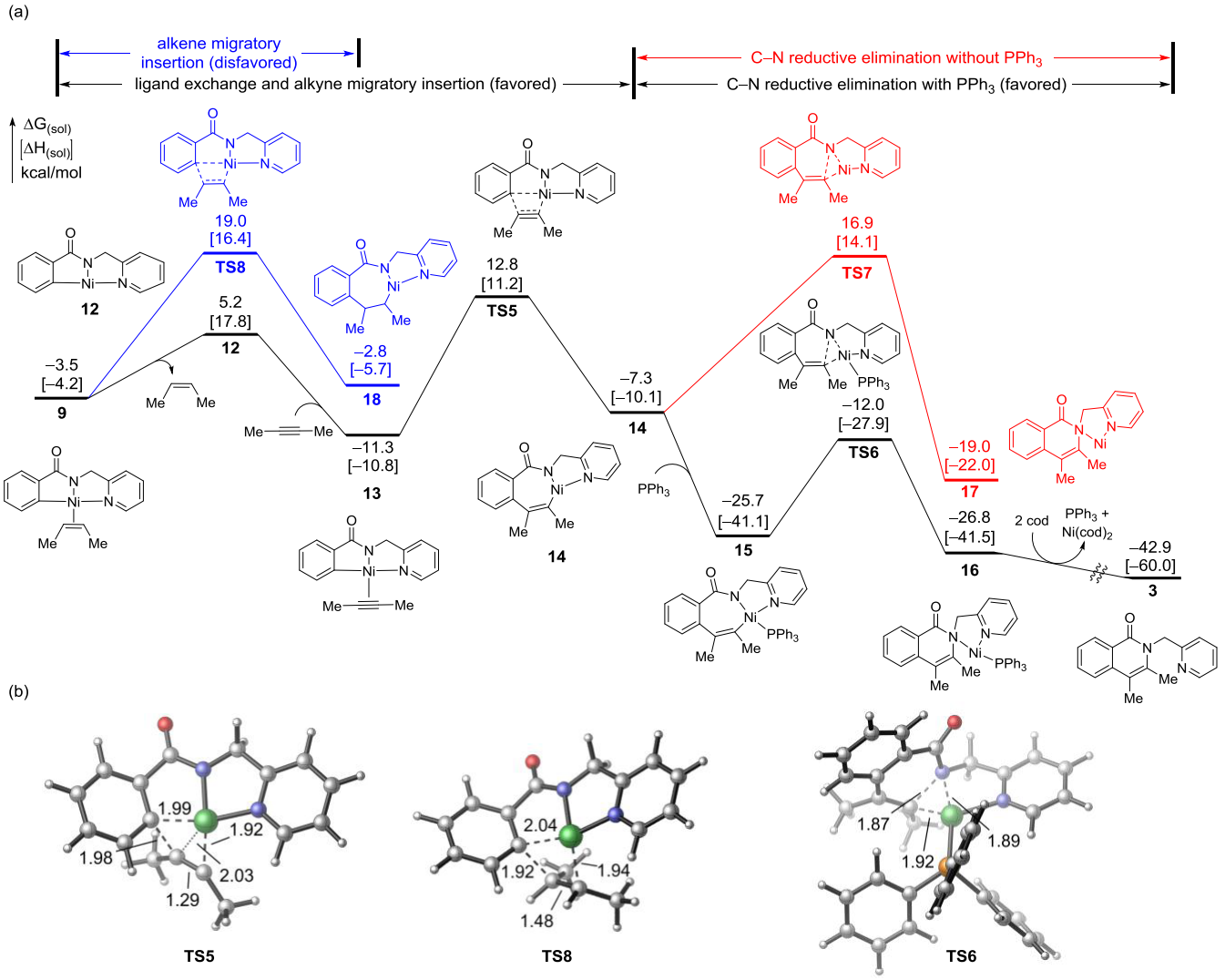

Figure 2. Mechanisms of the C−C and C−N bond formation steps from the nickelacycle intermediate **9**. (a) Computed reaction energy profiles of C−C and C−N bond formation mechanisms. (b) Optimized structures of transition states with select bond distances shown in Å. All energies are with respect to the separate reactants and $Ni(cod)_2$.

higher than the corresponding C−N bond reductive elimination using the 2-pyridinylmethylamine directing group (**TS6**). In **TS6**, the five-membered *N*,*N*-chelate adapts an envelope conformation in which the sp^3 carbon (C1) is puckered out of plane. This allows the forming C−N bond to be coplanar with the pyridine N and the PPh_3 ligand such that the Ni(II) center can adopt a less-distorted square planar geometry. On the other hand, the rigid 8-aminoquinoline directing group leads to greater distortion of the fused rings in **TS9** that makes the C−N bond reductive elimination less effective.[37]

In summary, the most favorable mechanism in the Ni-catalyzed *ortho* C(sp^2)−H oxidative cycloaddition of aromatic amide **1** and internal alkyne **2** proceeds by oxidative addition into the amide N−H bond to form Ni(II)-hydride **5**, followed by alkyne insertion to form an alkenyl-Ni(II) complex **8**. The agostic interaction with the *ortho* C−H bond in the σ-complex **8** promotes C−H metalation via a σ-CAM mechanism to afford alkene-bound five-membered nickelacycle. Insertion of another alkyne molecule and phosphine-promoted C−N reductive elimination afford the isoquinolone product and regenerate the Ni(0) catalyst.

2.4. Origin of Regioselectivity with Unsymmetrical Internal Aryl Alkynes. We next investigated the origin of the high levels of regioselectivity in reactions with unsymmetrical internal alkynes. When phenylalkylacetylenes are used as coupling partners, this oxidative cycloaddition reaction tolerates bulky alkyl substituents, such as *tert*-butyl, on the alkyne (Scheme 4). Interestingly, the major regioisomeric pathway involves formation of a new C−C bond with the more sterically demanding alkyne terminus. In addition, a greater regioselectivity was observed when the size of the alkyl group increased from methyl to *tert*-butyl. To investigate the origin of this "counter-steric" regioselectivity, we calculated the regioselectivity-determining alkyne insertion pathways with phenylalkylacetylenes **23** and **24** (Table 1).

In the reaction with 1-phenyl-1-propyne (**23**, R = Me), the alkyne insertion transition state (**TS-10A**) leading to the major regioisomer **A** is preferred by 1.6 kcal/mol, in good agreement with experimental regioselectivity (entry 1). The origin of this preference is attributed to the stabilization of the partial negative charge on the α-carbon of the forming Ni−C bond by the terminal phenyl group in **TS-10A**.[38] In the reaction with phenyl-*t*-butylacetylene (**24**, R = *t*-Bu), the major regioiso-

DOI: 10.1021/acsomega.9b00030
ACS Omega 2019, 4, 5209−5220

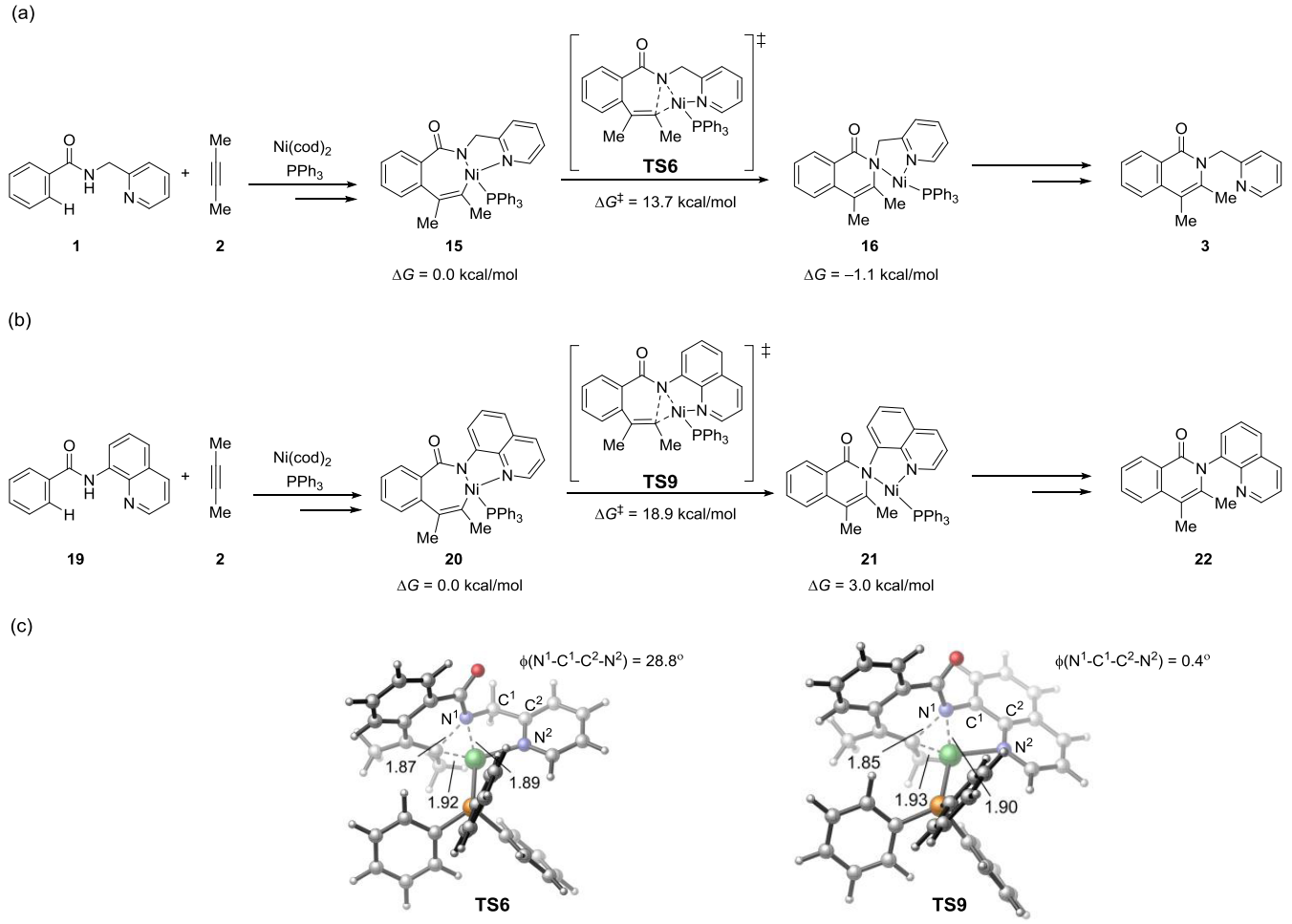

Figure 3. Effects of directing group on the C−N bond reductive elimination. (a) C−N reductive elimination with 2-pyridinylmethylamine directing group. (b) C−N reductive elimination with 8-aminoquinoline directing group. (c) Optimized structures of C−N reductive elimination transition states with select bond distances in angstrom (Å) and bond angles shown in degree. All energies are with respect to the phosphine-bound seven-membered nickelacycles **15** and **20**.

Scheme 4. Experimentally Observed Regioselectivity with Internal Aryl Alkynes[12]

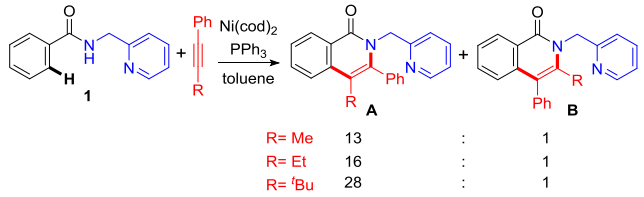

meric transition state **TS-11A** is stabilized by a similar electronic effect. **TS-11A** and **TS-10A** have almost identical activation barriers with respect to the corresponding π-alkyne complexes. Therefore, the reactivity of this migratory insertion is not sensitive to the steric bulk of the terminal alkyne substituent (R) adjacent to the forming C−C bond. The four-membered cyclic alkyne migration transition states **TS-11A** and **TS-10A** are not planar; the alkyl group (R) on the alkyne points out of the plane of the nickelacycle (Figure 4). As such, the steric repulsions between R and the nickelacycle in both transition states are diminished. On the other hand, in the minor regioisomeric transition state **TS-11B**, the bulky *tert*-Bu substituent is placed coplanar with the nickelacycle to achieve a square planar geometry of Ni(II). As such, substantial steric repulsions between the *tert*-Bu and the 2-pyridinylmethylamine directing group are observed in **TS-11B**. This steric effect makes the *tert*-Bu-substituted **TS-11B** 1.5 kcal/mol less stable than the Me-substituted **TS-10B** and thus leads to an increased regioselectivity ($\Delta\Delta G^{\ddagger}$ = 3.8 kcal/mol) when phenyl-*t*-butylacetylene (**24**) was used as the coupling partner.

2.5. Mechanism of Cis−Trans Isomerization of the Alkene Byproduct. In the Ni-catalyzed C−H bond functionalization of amide **1** with diphenylacetylene, *trans*-stilbene was produced in 81% yield.[12] The alkyne-promoted σ-CAM process discussed above forms *cis*-alkenes rather than the *trans*-isomers. As such, a cis-to-trans alkene isomerization must be operational. Because nickel hydride complexes are known to catalyze alkene isomerization reactions,[27a] we surmised that Ni(II)-hydride intermediate **5** in the main catalytic cycle may serve as a catalyst to promote the cis−trans isomerization. The reaction energy profile of this pathway was calculated (Figure 5).

Ligand exchange of PPh_3 in Ni(II)-hydride **5** with *cis*-2-butene forms complex **25**, which then undergoes alkene migratory insertion to form β-agostic alkyl-Ni(II) complex **27**.[39] From **27**, β-hydride elimination with a different C−H bond forms the *trans*-2-butene-bound Ni(II)-hydride **28**, which upon ligand exchange with PPh_3 extrudes the *trans*-2-butene byproduct. The cis−trans isomerization process in this

DOI: 10.1021/acsomega.9b00030
ACS Omega 2019, 4, 5209−5220

Table 1. Regioselectivity in Reactions with Unsymmetrical Alkynes[a]

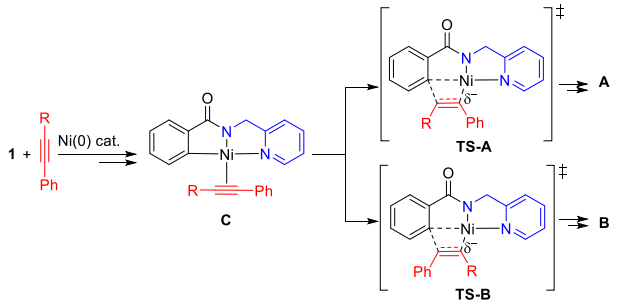

entry	alkyne	TS-A $\Delta G^{\ddagger}$ [$\Delta H^{\ddagger}$][a]	TS-B $\Delta G^{\ddagger}$ [$\Delta H^{\ddagger}$][a]	experimental selectivity (A : B)
1	Me—≡—Ph **23**	22.8 [20.5]	24.4 [22.0]	13:1
2	^{t}Bu—≡—Ph **24**	22.1 [19.4]	25.9 [23.9]	28:1

[a]Gibbs free energy and enthalpy of activation in the alkyne insertion step. All energies are in kcal/mol with respect to the alkyne-bound nickelacycle **C**.

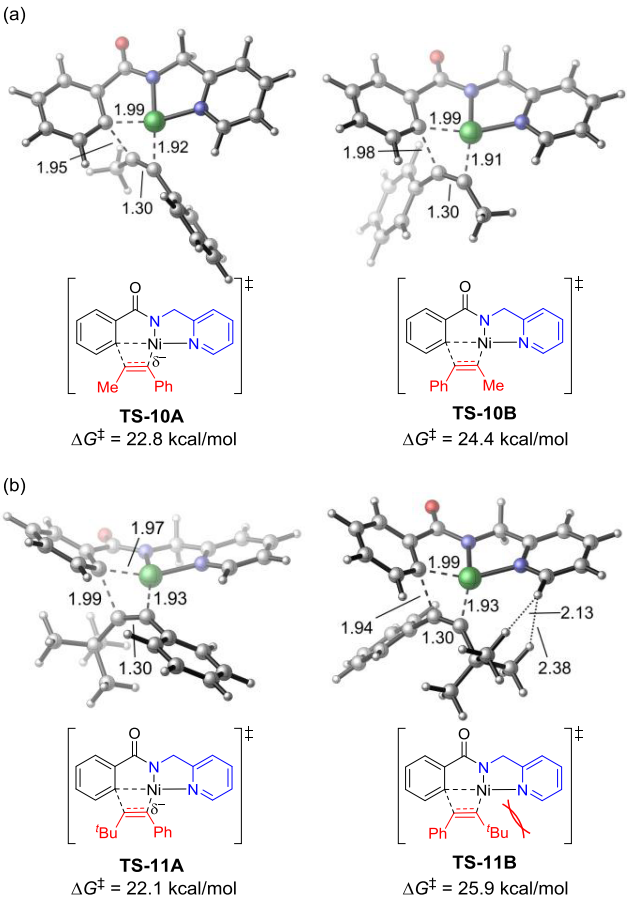

Figure 4. Regioselectivity-determining insertion transition states with (a) alkyne **23** and (b) alkyne **24**.

off-cycle pathway is kinetically feasible and thermodynamically exergonic by 0.9 kcal/mol. The presence of PPh_3 ligand does not significantly inhibit the reaction because the ligand exchange of PPh_3 with alkene is only uphill by about 11 kcal/mol. In addition, coordination to a PPh_3 ligand to form **26** does not stabilize the alkyl-Ni(II) intermediate **27**. Taken together, the computed reaction energy profile indicates that the Ni(II)-hydride intermediate **5** is a competent catalyst for the isomerization of *cis*-alkenes to the experimentally observed *trans*-alkene byproducts. These results further support the formation of Ni(II)-hydride complex in the main catalytic cycle.

3. CONCLUSIONS

The reaction mechanism of Ni-catalyzed *ortho* C(sp^2)−H oxidative cycloaddition of aromatic amides with internal alkynes containing 2-pyridinylmethylamine directing group was investigated using DFT calculations. The catalytic cycle begins by oxidative addition of the amide N−H bond to form a Ni(II)-hydride complex. The subsequent C−H metalation process occurs via a unique σ-complex-assisted metathesis (σ-CAM) mechanism where the internal alkyne acts as a hydrogen acceptor. This contrasts with the CMD mechanism that is usually involved in the Ni-catalyzed C−H metalation in the presence of carboxylate or carbonate bases. The alkyne plays significant roles in promoting the σ-CAM pathway both thermodynamically as a H_2 acceptor and kinetically. Because the Ni(II)-hydride intermediate is thermodynamically unstable, σ-CAM from the Ni(II)-hydride requires a high overall barrier. On the other hand, in the presence of the alkyne, the Ni(II)-hydride is converted to a more stable alkenyl-Ni(II) species, which then undergoes more facile σ-CAM.

The subsequent reaction with the alkene-bound nickelacycle proceeds via an exergonic ligand exchange with another molecule of alkyne, followed by alkyne insertion to form a seven-membered nickelacycle. The insertion of the alkene is less favorable. The alkyne migratory insertion occurs via a nonplanar four-membered cyclic transition state, in which the steric repulsion about the forming C−C bond is diminished. As such, this reaction tolerates alkynes with very bulky terminus and offers high regioselectivity to form the sterically more encumbered C−C bond. The C−N bond reductive elimination of the seven-membered nickelacycle is a key step to form the cyclic isoquinolone products. This C−N bond reductive elimination is promoted by a PPh_3 ligand and the flexible 2-pyridinylmethylamine directing group, which reduces the strain of the fused cyclic system in the reductive elimination transition state. The cis−trans isomerism of the alkene byproduct was also explored computationally. This process is catalyzed by a Ni(II)-hydride intermediate in the main catalytic cycle.

We expect that the mechanistic insights from this study, in particular, the unique roles of alkynes to promote the σ-CAM pathway, will aid in the development of other transition-metal-catalyzed C−H functionalization reactions with alkynes.

4. COMPUTATIONAL METHODS

All calculations were performed using Gaussian 09.[40] Images of the 3D structures of molecules were generated using CYLview.[41] Geometry optimizations and vibrational frequency calculations were performed using the B3LYP[42] functional in gas phase with the LANL2DZ effective core potential basis set

DOI: 10.1021/acsomega.9b00030
ACS Omega 2019, 4, 5209−5220

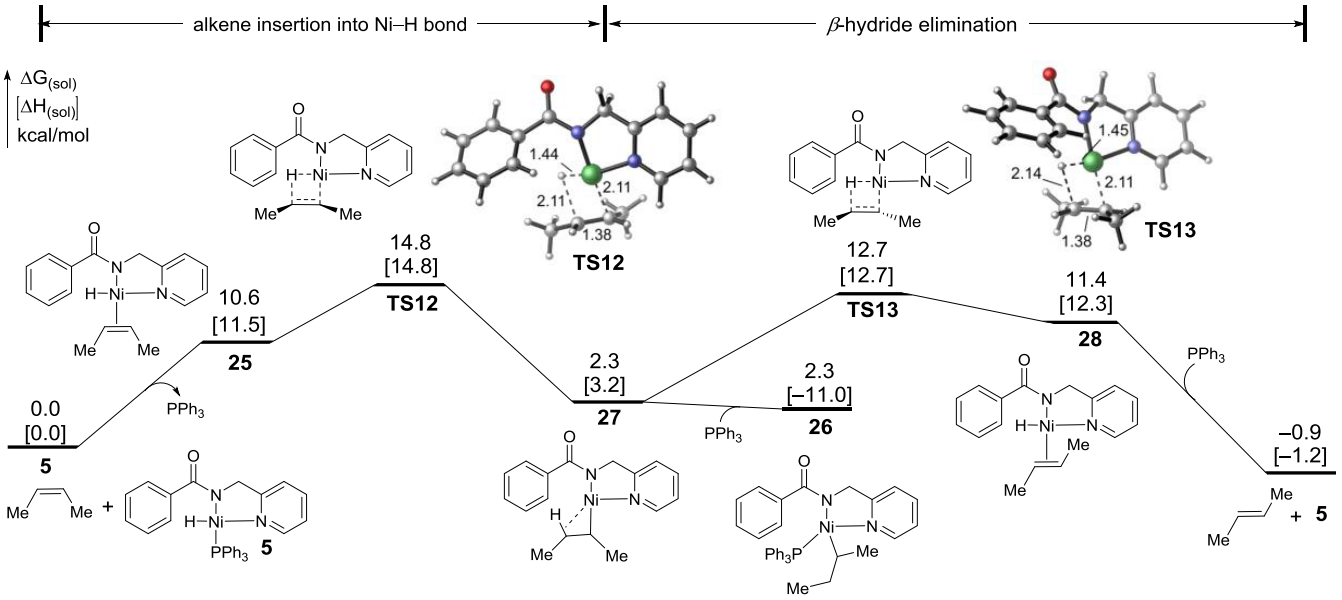

Figure 5. Reaction energy profile of the Ni(II)-hydride-catalyzed isomerization of *cis*-2-butene to *trans*-2-butene. All energies are with respect to the Ni(II)-hydride complex **5** and *cis*-2-butene.

for nickel and the 6-31G(d) basis set for other atoms. The nature of all stationary points was confirmed by the number of imaginary frequencies. All minima have zero imaginary frequency, and all transition states have only one imaginary frequency. IRC calculations were carried out for alkene and alkyne insertion transition states and for σ-CAM transition states to confirm that the transition state structures connected to the appropriate intermediates. Single-point energy calculations were carried out using the M06[43] functional and the SDD basis set for Ni and 6-311+G(d,p) for other atoms. The SMD[44] solvation model was used in the single-point energy calculations to incorporate solvent effects with toluene as the solvent. Thermal corrections to the Gibbs free energies and enthalpies were calculated using the harmonic oscillator approximation at 298.15 K.

■ ASSOCIATED CONTENT

Supporting Information

The Supporting Information is available free of charge on the ACS Publications website at DOI: 10.1021/acsomega.9b00030.

Reaction energy profiles of amide N–H oxidative addition with different ligands (Figure S1), alternative C–H metalation mechanisms with *cis*-2-butene (Figure S2), via σ-bond metathesis of phosphine-bound Ni(II)-hydride (Figure S3), via oxidative addition to Ni(0) (Figure S4), via deprotonation by the amide N (Figure S5), and C–N reductive elimination with model substrates (Figure S6); Cartesian coordinates of optimized geometries (PDF)

■ AUTHOR INFORMATION

Corresponding Author

*E-mail: pengliu@pitt.edu.

ORCID

Peng Liu: 0000-0002-8188-632X

Notes

The authors declare no competing financial interest.

■ ACKNOWLEDGMENTS

The authors acknowledge the NSF (CHE-1654122) for funding. Calculations were performed at the Center for Research Computing at the University of Pittsburgh and the Extreme Science and Engineering Discovery Environment (XSEDE) supported by NSF.

■ REFERENCES

(1) (a) Godula, K.; Sames, D. C-H Bond Functionalization in Complex Organic Synthesis. *Science* **2006**, *312*, 67–72. (b) Albrecht, M. Cyclometalation Using d-Block Transition Metals: Fundamental Aspects and Recent Trends. *Chem. Rev.* **2010**, *110*, 576–623. (c) Balcells, D.; Clot, E.; Eisenstein, O. C–H Bond Activation in Transition Metal Species from a Computational Perspective. *Chem. Rev.* **2010**, *110*, 749–823. (d) Yeung, C. S.; Dong, V. M. Catalytic Dehydrogenative Cross-Coupling: Forming Carbon–Carbon Bonds by Oxidizing Two Carbon–Hydrogen Bonds. *Chem. Rev.* **2011**, *111*, 1215–1292. (e) Brückl, T.; Baxter, R. D.; Ishihara, Y.; Baran, P. S. Innate and Guided C–H Functionalization Logic. *Acc. Chem. Res.* **2012**, *45*, 826–839. (f) Pototschnig, G.; Maulide, N.; Schnürch, M. Direct Functionalization of C–H Bonds by Iron, Nickel, and Cobalt Catalysis. *Chem. Eur. J.* **2017**, *23*, 9206–9232. (g) Chen, Z.; Wang, B.; Zhang, J.; Yu, W.; Liu, Z.; Zhang, Y. Transition metal-catalyzed C–H bond functionalizations by the use of diverse directing groups. *Org. Chem. Front.* **2015**, *2*, 1107–1295. (h) Wencel-Delord, J.; Dröge, T.; Liu, F.; Glorius, F. Towards mild metal-catalyzed C–H bond activation. *Chem. Soc. Rev.* **2011**, *40*, 4740–4761. (i) Davies, H. M. L.; Morton, D. Recent Advances in C–H Functionalization. *J. Org. Chem.* **2016**, *81*, 343–350.

(2) (a) Zaitsev, V. G.; Shabashov, D.; Daugulis, O. Highly Regioselective Arylation of sp3 C–H Bonds Catalyzed by Palladium Acetate. *J. Am. Chem. Soc.* **2005**, *127*, 13154–13155. (b) Nadres, E. T.; Santos, G. I. F.; Shabashov, D.; Daugulis, O. Scope and Limitations of Auxiliary-Assisted, Palladium-Catalyzed Arylation and Alkylation of sp2 and sp3 C–H Bonds. *J. Org. Chem.* **2013**, *78*, 9689–9714. (c) Daugulis, O.; Roane, J.; Tran, L. D. Bidentate, Monoanionic Auxiliary-Directed Functionalization of Carbon–Hydrogen Bonds. *Acc. Chem. Res.* **2015**, *48*, 1053–1064.

(3) For reviews on chelation-assisted C–H functionalization, see: (a) Rouquet, G.; Chatani, N. Catalytic Functionalization of C(sp2)–H and C(sp3)–H Bonds by Using Bidentate Directing Groups. *Angew. Chem., Int. Ed.* **2013**, *52*, 11726–11743. (b) Rit, R. K.; Yadav,

DOI: 10.1021/acsomega.9b00030
ACS Omega 2019, 4, 5209–5220

M. R.; Ghosh, K.; Sahoo, A. K. Reusable directing groups [8-aminoquinoline, picolinamide, sulfoximine] in C(sp3)−H bond activation: present and future. *Tetrahedron* **2015**, *71*, 4450−4459. (c) Yang, X.; Shan, G.; Wang, L.; Rao, Y. Recent advances in transition metal (Pd, Ni)-catalyzed C(sp3)−H bond activation with bidentate directing groups. *Tetrahedron Lett.* **2016**, *57*, 819−836. (d) He, R.; Huang, Z.-T.; Zheng, Q.-Y.; Wang, C. Isoquinoline skeleton synthesis via chelation-assisted C−H activation. *Tetrahedron Lett.* **2014**, *55*, 5705−5713.

(4) For reviews on Ni-catalyzed C−H functionalization, see: (a) Tasker, S. Z.; Standley, E. A.; Jamison, T. F. Recent advances in homogeneous nickel catalysis. *Nature* **2014**, *509*, 299−309. (b) Chatani, N. Nickel-Catalyzed C−H Bond Functionalization Utilizing an N,N′-Bidentate Directing Group. *Top. Organomet. Chem.* **2016**, *56*, 19−46. (c) Aihara, Y.; Wuelbern, J.; Chatani, N. The Nickel(II)-Catalyzed Direct Benzylation, Allylation, Alkylation, and Methylation of CH Bonds in Aromatic Amides Containing an 8-Aminoquinoline Moiety as the Directing Group. *Bull. Chem. Soc. Jpn.* **2015**, *88*, 438−446. (d) Castro, L. C. M.; Chatani, N. Nickel Catalysts/N,N′-Bidentate Directing Groups: An Excellent Partnership in Directed C−H Activation Reactions. *Chem. Lett.* **2015**, *44*, 410−421. (e) Cai, X.; Xie, B. Recent advances in nickel-catalyzed C−H bond functionalized reactions. *ARKIVOC* **2015**, *i*, 184. (f) Yamaguchi, J.; Muto, K.; Itami, K. Nickel-Catalyzed Aromatic C-H Functionalization. *Top. Curr. Chem.* **2016**, *374*, 55. (g) Yamaguchi, J.; Muto, K.; Itami, K. Recent Progress in Nickel-Catalyzed Biaryl Coupling. *Eur. J. Org. Chem.* **2013**, 19−30. (h) Khan, M. S.; Haque, A.; Al-Suti, M. K.; Raithby, P. R. Recent advances in the application of group-10 transition metal based catalysts in C-H activation and functionalization. *J. Organomet. Chem.* **2015**, *793*, 114−133. (i) Johnson, S. A. Nickel complexes for catalytic C−H bond functionalization. *Dalton Trans.* **2015**, *44*, 10905−10913.

(5) (a) Davies, D. L.; Donald, S. M. A.; Macgregor, S. A. Computational Study of the Mechanism of Cyclometalation by Palladium Acetate. *J. Am. Chem. Soc.* **2005**, *127*, 13754−13755. (b) Lapointe, D.; Fagnou, K. Computational Study of the Mechanism of Cyclometalation by Palladium Acetate. *Chem. Lett.* **2010**, *39*, 1118−1126. (c) Lafrance, M.; Gorelsky, S. I.; Fagnou, K. High-Yielding Palladium-Catalyzed Intramolecular Alkane Arylation: Reaction Development and Mechanistic Studies. *J. Am. Chem. Soc.* **2007**, *129*, 14570−14571. (d) Gorelsky, S. I.; Lapointe, D.; Fagnou, K. Analysis of the Concerted Metalation-Deprotonation Mechanism in Palladium-Catalyzed Direct Arylation Across a Broad Range of Aromatic Substrates. *J. Am. Chem. Soc.* **2008**, *130*, 10848−10849. (e) Guihaumé, J.; Clot, E.; Eisenstein, O.; Perutz, R. N. Importance of palladium−carbon bond energies in direct arylation of polyfluorinated benzenes. *Dalton Trans.* **2010**, *39*, 10510−10519. (f) Gorelsky, S. I.; Lapointe, D.; Fagnou, K. Analysis of the Palladium-Catalyzed (Aromatic)C−H Bond Metalation−Deprotonation Mechanism Spanning the Entire Spectrum of Arenes. *J. Org. Chem.* **2012**, *77*, 658−668. (g) Petit, A.; Flygare, J.; Miller, A. T.; Winkel, G.; Ess, D. H. Transition-State Metal Aryl Bond Stability Determines Regioselectivity in Palladium Acetate Mediated C−H Bond Activation of Heteroarenes. *Org. Lett.* **2012**, *14*, 3680−3683. (h) Dang, Y.; Qu, S.; Nelson, J. W.; Pham, H. D.; Wang, Z.-X.; Wang, X. The Mechanism of a Ligand-Promoted C(sp3)−H Activation and Arylation Reaction via Palladium Catalysis: Theoretical Demonstration of a Pd(II)/Pd(IV) Redox Manifold. *J. Am. Chem. Soc.* **2015**, *137*, 2006−2014. (i) Dang, Y.; Deng, X.; Guo, J.; Song, C.; Hu, W.; Wang, Z.-X. Unveiling Secrets of Overcoming the "Heteroatom Problem" in Palladium-Catalyzed Aerobic C−H Functionalization of Heterocycles: A DFT Mechanistic Study. *J. Am. Chem. Soc.* **2016**, *138*, 2712−2723. (j) Davies, D. L.; Macgregor, S. A.; McMullin, C. L. Computational Studies of Carboxylate-Assisted C−H Activation and Functionalization at Group 8−10 Transition Metal Centers. *Chem. Rev.* **2017**, *117*, 8649−8709. (k) García-Cuadrado, D.; Braga, A. A. C.; Maseras, F.; Echavarren, A. M. Proton Abstraction Mechanism for the Palladium-Catalyzed Intramolecular Arylation. *J. Am. Chem. Soc.* **2006**, *128*, 1066−1067. (l) Lafrance, M.; Rowley, C. N.; Woo, T. K.; Fagnou, K. Catalytic Intermolecular Direct Arylation of Perfluorobenzenes. *J. Am. Chem. Soc.* **2006**, *128*, 8754−8756. (m) Pascual, S.; Mendoza, P.; Braga, A. A. C.; Maseras, F.; Echavarren, A. M. Bidentate phosphines as ligands in the palladium-catalyzed intramolecular arylation: the intermolecular base-assisted proton abstraction mechanism. *Tetrahedron* **2008**, *64*, 6021−6029. (n) Kefalidis, C. E.; Baudoin, O.; Clot, E. DFT study of the mechanism of benzocyclobutene formation by palladium-catalysed C(sp3)−H activation: role of the nature of the base and the phosphine. *Dalton Trans.* **2010**, *39*, 10528−10535. (o) Korenaga, T.; Suzuki, N.; Sueda, M.; Shimada, K. Ligand effect on direct arylation by CMD process. *J. Organomet. Chem.* **2015**, *780*, 63−69. (p) Holstein, P. M.; Vogler, M.; Larini, P.; Pilet, G.; Clot, E.; Baudoin, O. Efficient Pd0-Catalyzed Asymmetric Activation of Primary and Secondary C−H Bonds Enabled by Modular Binepine Ligands and Carbonate Bases. *ACS Catal.* **2015**, *5*, 4300−4308.

(6) Gensch, T.; Hopkinson, M. N.; Glorius, F.; Wencel-Delord, J. Mild metal-catalyzed C−H activation: examples and concepts. *Chem. Soc. Rev.* **2016**, *45*, 2900−2936.

(7) Perutz, R. N.; Sabo-Etienne, S. The σ-CAM Mechanism: σ-Complexes as the Basis of σ-Bond Metathesis at Late-Transition-Metal Centers. *Angew. Chem., Int. Ed.* **2007**, *46*, 2578−2592.

(8) (a) Guihaumé, J.; Halbert, S.; Eisenstein, O.; Perutz, R. N. Hydrofluoroarylation of Alkynes with Ni Catalysts. C−H Activation via Ligand-to-Ligand Hydrogen Transfer, an Alternative to Oxidative Addition. *Organometallics* **2012**, *31*, 1300−1314. (b) Tang, S.; Eisenstein, O.; Nakao, Y.; Sakaki, S. Aromatic C−H σ-Bond Activation by Ni0, Pd0, and Pt0 Alkene Complexes: Concerted Oxidative Addition to Metal vs Ligand-to-Ligand H Transfer Mechanism. *Organometallics* **2017**, *36*, 2761−2771. (c) Yamazaki, K.; Obata, A.; Sasagawa, A.; Ano, Y.; Chatani, N. Computational Mechanistic Study on the Nickel-Catalyzed C−H/N−H Oxidative Annulation of Aromatic Amides with Alkynes: The Role of the Nickel (0) Ate Complex. *Organometallics* **2019**, *38*, 248−255.

(9) (a) Shibata, K.; Hasegawa, N.; Fukumoto, Y.; Chatani, N. Ruthenium-Catalyzed Carbonylation of ortho C−H Bonds in Arylacetamides: C−H Bond Activation Utilizing a Bidentate-Chelation System. *ChemCatChem* **2012**, *4*, 1733−1736. (b) Hasegawa, N.; Shibata, K.; Charra, V.; Inoue, S.; Fukumoto, Y.; Chatani, N. Ruthenium-catalyzed cyclocarbonylation of aliphatic amides through the regioselective activation of unactivated C(sp3)−H bonds. *Tetrahedron* **2013**, *69*, 4466−4472. (c) Misal Castro, L. C.; Obata, A.; Aihara, Y.; Chatani, N. Chelation-Assisted Nickel-Catalyzed Oxidative Annulation via Double C−H Activation/Alkyne Insertion Reaction. *Chem. Eur. J.* **2016**, *22*, 1362−1367. (d) He, Z.; Huang, Y. Diverting C−H Annulation Pathways: Nickel-Catalyzed Dehydrogenative Homologation of Aromatic Amides. *ACS Catal.* **2016**, *6*, 7814−7823.

(10) For computational studies of Ni-catalyzed C−H functionalization using *N,N*-bidentate strategy, see: (a) Tang, H.; Zhou, B.; Huang, X.-R.; Wang, C.; Yao, J.; Chen, H. Origins of Selective C(sp2)−H Activation Using Transition Metal Complexes with N,N-Bidentate Directing Groups: A Combined Theoretical−Experimental Study. *ACS Catal.* **2014**, *4*, 649−656. (b) Tang, H.; Huang, X.-R.; Yao, J.; Chen, H. Understanding the Effects of Bidentate Directing Groups: A Unified Rationale for sp2 and sp3 C−H Bond Activations. *J. Org. Chem.* **2015**, *80*, 4672−4682. (c) Xu, Z.-Y.; Jiang, Y.-Y.; Yu, H.-Z.; Fu, Y. Mechanism of Nickel(II)-Catalyzed Oxidative C(sp2)−H/C-(sp3)−H Coupling of Benzamides and Toluene Derivatives. *Chem. - Asian J.* **2015**, *10*, 2479−2483. (d) Singh, S.; K, S.; Sunoj, R. B. Aliphatic C(sp3)−H Bond Activation Using Nickel Catalysis: Mechanistic Insights on Regioselective Arylation. *J. Org. Chem.* **2017**, *82*, 9619−9626. (e) Omer, H. M.; Liu, P. Computational Study of Ni-Catalyzed C−H Functionalization: Factors That Control the Competition of Oxidative Addition and Radical Pathways. *J. Am. Chem. Soc.* **2017**, *139*, 9909−9920. (f) Haines, B. E.; Yu, J.-Q.; Musaev, D. G. The mechanism of directed Ni(II)-catalyzed C−H iodination with molecular iodine. *Chem. Sci.* **2018**, *9*, 1144−1154. (g) Li, Y.; Zou, L.; Bai, R.; Lan, Y. Ni(I)−Ni(III) vs. Ni(II)−Ni(IV):

DOI: 10.1021/acsomega.9b00030
ACS Omega 2019, 4, 5209−5220

mechanistic study of Ni-catalyzed alkylation of benzamides with alkyl halides. *Org. Chem. Front.* **2018**, *5*, 615−622.
(11) For computational studies of other metal-catalyzed C−H functionalization using *N,N*-bidentate group strategy, see: (a) Cross, W. B.; Hope, E. G.; Lin, Y.-H.; Macgregor, S. A.; Singh, K.; Solan, G. A.; Yahyaa, N. N,N-Chelate-control on the regioselectivity in acetate-assisted C−H activation. *Chem. Commun.* **2013**, *49*, 1918−1920. (b) Huang, L.; Li, Q.; Wang, C.; Qi, C. Palladium(II)-Catalyzed Regioselective Arylation of Naphthylamides with Aryl Iodides Utilizing a Quinolinamide Bidentate System. *J. Org. Chem.* **2013**, *78*, 3030−3038. (c) Wei, Y.; Tang, H.; Cong, X.; Rao, B.; Wu, C.; Zeng, X. Pd(II)-Catalyzed Intermolecular Arylation of Unactivated C(sp3)−H Bonds with Aryl Bromides Enabled by 8-Aminoquinoline Auxiliary. *Org. Lett.* **2014**, *16*, 2248−2251. (d) Shan, C.; Luo, X.; Qi, X.; Liu, S.; Li, Y.; Lan, Y. Mechanism of Ruthenium-Catalyzed Direct Arylation of C−H Bonds in Aromatic Amides: A Computational Study. *Organometallics* **2016**, *35*, 1440−1445. (e) Chen, C.; Hao, Y.; Zhang, T.-Y.; Pan, J.-L.; Ding, J.; Xiang, H.-Y.; Wang, M.; Ding, T.-M.; Duan, A.; Zhang, S.-Y. Computational and experimental studies on copper-mediated selective cascade C−H/N−H annulation of electron-deficient acrylamide with arynes. *Chem. Commun.* **2019**, *55*, 755−758. (f) Dewyer, A. L.; Zimmerman, P. M. Simulated Mechanism for Palladium Catalyzed, Directed γ-Arylation of Piperidine. *ACS Catal.* **2017**, *7*, 5466−5477.
(12) Shiota, H.; Ano, Y.; Aihara, Y.; Fukumoto, Y.; Chatani, N. Nickel-Catalyzed Chelation-Assisted Transformations Involving Ortho C−H Bond Activation: Regioselective Oxidative Cycloaddition of Aromatic Amides to Alkynes. *J. Am. Chem. Soc.* **2011**, *133*, 14952−14955.
(13) For a recent computational study on this reaction, see: Zhang, X.; Zhao, Q.; Fan, J.-Q.; Chen, D.-Z.; Liu, J.-B. A computational mechanistic study of Ni(0)-catalyzed annulation of aromatic amides with alkynes: the effects of directing groups. *Org. Chem. Front.* **2019**, DOI: 10.1039/C8QO01310A.
(14) For select examples of chelation-assisted Ni-catalyzed C−H arylation, see: (a) Aihara, Y.; Chatani, N. Nickel-Catalyzed Direct Arylation of C(sp3)−H Bonds in Aliphatic Amides via Bidentate-Chelation Assistance. *J. Am. Chem. Soc.* **2014**, *136*, 898−901. (b) Yokota, A.; Aihara, Y.; Chatani, N. Nickel(II)-Catalyzed Direct Arylation of C−H Bonds in Aromatic Amides Containing an 8-Aminoquinoline Moiety as a Directing Group. *J. Org. Chem.* **2014**, *79*, 11922−11932. (c) Li, M.; Dong, J.; Huang, X.; Li, K.; Wu, Q.; Song, F.; You, J. Nickel-catalyzed chelation-assisted direct arylation of unactivated C(sp3)−H bonds with aryl halides. *Chem. Commun.* **2014**, *50*, 3944−3946.
(15) For select examples of chelation-assisted Ni-catalyzed C−H alkylation, see: (a) Kubo, T.; Chatani, N. Dicumyl Peroxide as a Methylating Reagent in the Ni-Catalyzed Methylation of Ortho C−H Bonds in Aromatic Amides. *Org. Lett.* **2016**, *18*, 1698−1701. (b) Aihara, Y.; Chatani, N. Nickel-Catalyzed Direct Alkylation of C−H Bonds in Benzamides and Acrylamides with Functionalized Alkyl Halides via Bidentate-Chelation Assistance. *J. Am. Chem. Soc.* **2013**, *135*, 5308−5311. (c) Wu, X.; Zhao, Y.; Ge, H. Nickel-Catalyzed Site-Selective Alkylation of Unactivated C(sp3)−H Bonds. *J. Am. Chem. Soc.* **2014**, *136*, 1789−1792. (d) Song, W.; Lackner, S.; Ackermann, L. Nickel-Catalyzed C−H Alkylations: Direct Secondary Alkylations and Trifluoroethylations of Arenes. *Angew. Chem., Int. Ed.* **2014**, *53*, 2477−2480.
(16) For select examples of chelation-assisted Ni-catalyzed C−H benzylation, see: (a) Aihara, Y.; Tobisu, M.; Fukumoto, Y.; Chatani, N. Ni(II)-Catalyzed Oxidative Coupling between C(sp2)−H in Benzamides and C(sp3)−H in Toluene Derivatives. *J. Am. Chem. Soc.* **2014**, *136*, 15509−15512. (b) Soni, V.; Khake, S. M.; Punji, B. Nickel-Catalyzed C(sp2)−H/C(sp3)−H Oxidative Coupling of Indoles with Toluene Derivatives. *ACS Catal.* **2017**, *7*, 4202−4208.
(17) For select examples of chelation-assisted Ni-catalyzed C−H thiolation, see: (a) Yan, S.-Y.; Liu, Y.-J.; Liu, B.; Liu, Y.-H.; Shi, B.-F. Nickel-catalyzed thiolation of unactivated aryl C−H bonds: efficient access to diverse aryl sulfides. *Chem. Commun.* **2015**, *51*, 4069−4072. (b) Yan, S.-Y.; Liu, Y.-J.; Liu, B.; Liu, Y.-H.; Zhang, Z.-Z.; Shi, B.-F. Nickel-catalyzed direct thiolation of unactivated C(sp3)−H bonds with disulfides. *Chem. Commun.* **2015**, *51*, 7341−7344. (c) Lin, C.; Li, D.; Wang, B.; Yao, J.; Zhang, Y. Direct ortho-Thiolation of Arenes and Alkenes by Nickel Catalysis. *Org. Lett.* **2015**, *17*, 1328−1331. (d) Reddy, V. P.; Qiu, R.; Iwasaki, T.; Kambe, N. Nickel-catalyzed synthesis of diaryl sulfides and sulfones via C−H bond functionalization of arylamides. *Org. Biomol. Chem.* **2015**, *13*, 6803−6813.
(18) Aihara, Y.; Chatani, N. Nickel-Catalyzed Reaction of C−H Bonds in Amides with I2: ortho-Iodination via the Cleavage of C(sp2)−H Bonds and Oxidative Cyclization to β-Lactams via the Cleavage of C(sp3)−H Bonds. *ACS Catal.* **2016**, *6*, 4323−4329.
(19) Nakao, Y.; Morita, E.; Idei, H.; Hiyama, T. Dehydrogenative [4 + 2] Cycloaddition of Formamides with Alkynes through Double C−H Activation. *J. Am. Chem. Soc.* **2011**, *133*, 3264−3267.
(20) (a) Lin, C.; Chen, Z.; Liu, Z.; Zhang, Y. Nickel-Catalyzed Stereoselective Alkenylation of C(sp3)−H Bonds with Terminal Alkynes. *Org. Lett.* **2017**, *19*, 850−853. (b) Li, M.; Yang, Y.; Zhou, D.; Wan, D.; You, J. Nickel-Catalyzed Addition-Type Alkenylation of Unactivated, Aliphatic C−H Bonds with Alkynes: A Concise Route to Polysubstituted γ-Butyrolactones. *Org. Lett.* **2015**, *17*, 2546−2549. (c) Maity, S.; Agasti, S.; Earsad, A. M.; Hazra, A.; Maiti, D. Nickel-Catalyzed Insertion of Alkynes and Electron-Deficient Olefins into Unactivated sp3 C−H Bonds. *Chem. - Eur. J.* **2015**, *21*, 11320−11324. (d) Liu, Y.-H.; Liu, Y.-J.; Yan, S.-Y.; Shi, B.-F. Ni(II)-catalyzed dehydrative alkynylation of unactivated (hetero)aryl C−H bonds using oxygen: a user-friendly approach. *Chem. Commun.* **2015**, *51*, 11650−11653.
(21) For C−H functionalization reactions where alkyne or alkene act as hydrogen acceptor, see: (a) Inoue, S.; Shiota, H.; Fukumoto, Y.; Chatani, N. Ruthenium-Catalyzed Carbonylation at Ortho C−H Bonds in Aromatic Amides Leading to Phthalimides: C−H Bond Activation Utilizing a Bidentate System. *J. Am. Chem. Soc.* **2009**, *131*, 6898−6899. (b) Hasegawa, N.; Charra, V.; Inoue, S.; Fukumoto, Y.; Chatani, N. Highly Regioselective Carbonylation of Unactivated C(sp3)−H Bonds by Ruthenium Carbonyl. *J. Am. Chem. Soc.* **2011**, *133*, 8070−8073. (c) Song, W.; Ackermann, L. Nickel-catalyzed alkyne annulation by anilines: versatile indole synthesis by C−H/N−H functionalization. *Chem. Commun.* **2013**, *49*, 6638−6640. (d) Obata, A.; Ano, Y.; Chatani, N. Nickel-catalyzed C−H/N−H annulation of aromatic amides with alkynes in the absence of a specific chelation system. *Chem. Sci.* **2017**, *8*, 6650−6655.
(22) For Rh-catalyzed C−H functionalization with internal alkyne, see: (a) Mochida, S.; Nobuyoshi, U.; Koji, H.; Tetsuya, S.; Masahiro, M. Rhodium-catalyzed Oxidative Coupling/Cyclization of Benzamides with Alkynes via C−H Bond Cleavage. *Chem. Lett.* **2010**, *39*, 744−746. (b) Hyster, T. K.; Rovis, T. Rhodium-Catalyzed Oxidative Cycloaddition of Benzamides and Alkynes via C−H/N−H Activation. *J. Am. Chem. Soc.* **2010**, *132*, 10565−10569. (c) Guimond, N.; Gorelsky, S. I.; Fagnou, K. Rhodium(III)-Catalyzed Heterocycle Synthesis Using an Internal Oxidant: Improved Reactivity and Mechanistic Studies. *J. Am. Chem. Soc.* **2011**, *133*, 6449−6457. (d) Hyster, T. K.; Rovis, T. An improved catalyst architecture for rhodium(III) catalyzed C−H activation and its application to pyridone synthesis. *Chem. Sci.* **2011**, *2*, 1606−1610. (e) Shan, G.; Flegel, J.; Li, H.; Merten, C.; Ziegler, S.; Antonchick, A. P.; Waldmann, H. C−H Bond Activation for the Synthesis of Heterocyclic Atropisomers Yields Hedgehog Pathway Inhibitors. *Angew. Chem., Int. Ed.* **2018**, *57*, 14250−14254. (f) Shibata, K.; Natsui, S.; Chatani, N. Rhodium-Catalyzed Alkenylation of C−H Bonds in Aromatic Amides with Alkynes. *Org. Lett.* **2017**, *19*, 2234−2237.
(23) For Ru-catalyzed C−H functionalization with internal alkynes, see: (a) Allu, S.; Swamy, K. C. K. Ruthenium-Catalyzed Synthesis of Isoquinolones with 8-Aminoquinoline as a Bidentate Directing Group in C−H Functionalization. *J. Org. Chem.* **2014**, *79*, 3963−3972. (b) Kaishap, P. P.; Duarah, G.; Chetiab, D.; Gogoi, S. Ru(II)-Catalyzed annulation of benzamidines and alkynes by C−H/N−H

DOI: 10.1021/acsomega.9b00030
ACS Omega 2019, 4, 5209−5220

activation: a facile synthesis of 1-aminoisoquinolines. *Org. Biomol. Chem.* **2017**, *15*, 3491−3498.
(24) For Pd-catalyzed C−H functionalization with internal alkynes, see: (a) Shu, Z.; Guo, Y.; Li, W.; Wang, B. Pd/C-catalyzed synthesis of N-aryl and N-alkyl isoquinolones via CH/NH activation. *Catal. Today* **2017**, *297*, 292−297. (b) Sharma, N.; Saha, R.; Parveen, N.; Sekar, G. Palladium-Nanoparticles-Catalyzed Oxidative Annulation of Benzamides with Alkynes for the Synthesis of Isoquinolones. *Adv. Synth. Catal.* **2017**, *359*, 1947−1958.
(25) For Co-catalyzed C−H functionalization with internal alkyne, see: (a) Grigorjeva, L.; Daugulis, O. Cobalt-catalyzed, aminoquinoline-directed C(sp^2)-H bond alkenylation by alkynes. *Angew. Chem., Int. Ed.* **2014**, *53*, 10209−10212. (b) Nguyen, T. T.; Grigorjeva, L.; Daugulis, O. Cobalt-Catalyzed, Aminoquinoline-Directed Functionalization of Phosphinic Amide sp2 C−H Bonds. *ACS Catal.* **2016**, *6*, 551−554. (c) Manoharan, R.; Jeganmohan, M. Cobalt-catalyzed cyclization of benzamides with alkynes: a facile route to isoquinolones with hydrogen evolution. *Org. Biomol. Chem.* **2018**, *16*, 8384−8389. (d) Zhai, S.; Qiu, S.; Chen, X.; Wu, J.; Zhao, H.; Tao, C.; Li, Y.; Cheng, B.; Wang, H.; Zhai, H. 2-(1-Methylhydrazinyl)pyridine as a reductively removable directing group in a cobalt-catalyzed C(sp2)−H bond alkenylation/annulation cascade. *Chem. Commun.* **2018**, *54*, 98−101.
(26) In the presence of a strong base, such as *t*-BuOK, N−H deprotonation would form a nickel(0) ate complex. A recent computational study indicates the subsequent C−H metalation from the nickel(0) ate complex occurs via a ligand-to-ligand hydrogen transfer mechanism. See ref 8c.
(27) For select reviews and crystal structures of Ni-hydride complexes, see: (a) Eberhardt, N. A.; Guan, H. Nickel Hydride Complexes. *Chem. Rev.* **2016**, *116*, 8373−8426. (b) Matson, E. M.; Martinez, G. E.; Ibrahim, A. D.; Jackson, B. J.; Bertke, J. A.; Fout, A. R. Nickel(II) Pincer Carbene Complexes: Oxidative Addition of an Aryl C−H Bond to Form a Ni(II) Hydride. *Organometallics* **2015**, *34*, 399−407. (c) Clement, N. D.; Cavell, K. J.; Jones, C.; Elsevier, C. J. Oxidative Addition of Imidazolium Salts to Ni0 and Pd0: Synthesis and Structural Characterization of Unusually Stable Metal−Hydride Complexes. *Angew. Chem., Int. Ed.* **2004**, *43*, 1277.
(28) Crabtree, R. H. Dihydrogen Complexation. *Chem. Rev.* **2016**, *116*, 8750−8769.
(29) (a) She, L.; Li, X.; Sun, H.; Ding, J.; Frey, M.; Klein, H.-F. Insertion of Alkynes into Ni−H Bonds: Synthesis of Novel Vinyl Nickel(II) and Dinuclear Vinyl Nickel(II) Complexes Containing a [P, S]-Ligand. *Organometallics* **2007**, *26*, 566−570. (b) Zhou, H.; Sun, H.; Zheng, T.; Zhang, S.; Li, X. Synthesis of Vinylnickel and Nickelacyclopropane Complexes Containing a Chelate [P,Se]-Ligand. *Eur. J. Inorg. Chem.* **2015**, 3139−3145. (c) Xue, B.; Sun, H.; Ren, S.; Li, X.; Fuhr, O. Vinyl/Phenyl Exchange Reaction within Vinyl Nickel Complexes Bearing Chelate [P, S]-Ligands. *Organometallics* **2017**, *36*, 4246−4255.
(30) An alternative pathway involving oxidative addition of *ortho* C(sp^2)−H bond with the Ni(0) catalyst was considered computationally. The barrier of the C−H oxidative addition is 19.5 kcal/mol with respect to amide **1** and Ni(cod)$_2$. However, the subsequent steps in this pathway were highly disfavored. Both alkyne insertion into Ni−H bond and N−H deprotonation to form the five-membered Ni(II) metallacycle **9** require very high activation barriers of 44.5 and 67.2 kcal/mol with respect to **1** and Ni(cod)$_2$, respectively. Based on these results, this oxidative addition pathway was ruled out (see Supporting Information for more details).
(31) (a) Brookhart, M.; Green, M. L. H.; Parkin, G. Agostic interactions in transition metal compounds. *Proc. Natl. Acad. Sci. USA* **2007**, *104*, 6908−6914. (b) Jongbloed, L. S.; García-Lopez, D.; Heck, R. V.; Siegler, M. A.; Carbo, J. J.; Vlugt, J. I. V. D. Arene C(sp2)-H Metalation at NiII Modeled with a Reactive PONCPh Ligand. *Inorg. Chem.* **2016**, *55*, 8041−8047. (c) Lein, M. Characterization of agostic interactions in theory and computation. *Coord. Chem. Rev.* **2009**, *253*, 625−634. (d) Etienne, M.; Weller, A. S. Intramolecular C−C agostic complexes: C−C sigma interactions by another name. *Chem. Soc. Rev.* **2014**, *43*, 242−259. (e) Beattie, D. D.; Bowes, E. G.; Drover, M. W.; Love, J. A.; Schafer, L. L. Oxidation State Dependent Coordination Modes: Accessing an Amidate-Supported Nickel(I) δ-bis(C−H) Agostic Complex. *Angew. Chem.* **2016**, *128*, 13484−13489. (f) Crabtree, R. H. Sigma Bonds as Ligand Donor Groups in Transition Metal Complexes. *The Chemical Bond III*; Mingos, D.M.P., Ed.; Springer International Publishing: Switzerland, 2015; Vol. *171*, pp 63−78.
(32) An alternatively pathway to form intermediate **11** from phosphine-bound Ni(II)-hydride complex **5** via σ-bond metathesis followed by PPh_3 decomplexation requires a much higher barrier (66.0 kcal/mol with respect to aromatic amide **1** and Ni(cod)$_2$ catalyst). This very high barrier is due to the absence of an agostic interaction and unfavorable steric effects of the additional PPh_3 ligand.
(33) PPh_3 coordination to intermediate **8** forms an off-cycle phosphine-bound alkenyl-Ni(II) complex **7**. Complex **7** is 11.2 kcal/mol more stable than **8**.
(34) (a) Another mechanism for C−H metalation involves σ-bond metathesis of the Ni−N bond in intermediate **8** with the *ortho* C−H bond to form a five-membered alkenyl-nickelacycle (see Supporting Information for details). This process requires an activation barrier of 39 kcal/mol with respect to the separate reactants and Ni(cod)$_2$, and thus can be ruled out. (b) In our calculations, we could not locate neither the transition state structure for the oxidative addition of the *ortho* C(sp^2)−H bond from alkenyl-Ni(II) complex **8** nor the resulting Ni(IV)-hydride complex. All attempts to locate these structures resulted in **TS3**, **8**, or **9**. Intrinsic reaction coordinate (IRC) calculations were carried out for **TS3** to confirm that it connects to complexes **8** and **9**.
(35) We also computationally considered the use of *cis*-2-butene rather than 2-butyne as the H_2 acceptor to promote the C−H metalation. In this alternatively pathway, the barrier of σ-bond metathesis is 34.8 kcal/mol with respect to the separate reactants and Ni(cod)$_2$, and thus this pathway is less favorable than that using alkyne as H_2 acceptor (see Supporting Information for details).
(36) McCarren, P. R.; Liu, P.; Cheong, P. H.-Y.; Jamison, T. F.; Houk, K. N. Mechanism and Transition-State Structures for Nickel-Catalyzed Reductive Alkyne−Aldehyde Coupling Reactions. *J. Am. Chem. Soc.* **2009**, *131*, 6654−6655.
(37) In addition, the N in 2-pyridinylmethylamine is a better donor that electronically promotes the reductive elimination via **TS6**.
(38) Liang, L.-C.; Pin-Shu Chien, P.-S.; Lee, P.-Y. Phosphorus and Olefin Substituent Effects on the Insertion Chemistry of Nickel(II) Hydride Complexes Containing Amido Diphosphine Ligands. *Organometallics* **2008**, *27*, 3082−3093.
(39) (a) Kogut, E.; Zeller, A.; Warren, T. H.; Strassner, T. Structure and Dynamics of Neutral β-H Agostic Nickel Alkyls: A Combined Experimental and Theoretical Study. *J. Am. Chem. Soc.* **2004**, *126*, 11984−11994. (b) Scherer, W.; Herz, V.; Brück, A.; Hauf, C.; Reiner, F.; Altmannshofer, S.; Leusser, D.; Stalke, D. The Nature of β-Agostic Bonding in Late-Transition-Metal Alkyl Complexes. *Angew. Chem., Int. Ed.* **2011**, *50*, 2845−2849.
(40) Frisch, M. J.; Trucks, G. W.; Schlegel, H. B.; Scuseria, G. E.; Robb, M. A.; Cheeseman, J. R.; Scalmani, G.; Barone, V.; Mennucci, B.; Petersson, G. A.; Nakatsuji, H.; Caricato, M.; Li, X.; Hratchian, H. P.; Izmaylov, A. F.; Bloino, J.; Zheng, G.; Sonnenberg, J. L.; Hada, M.; Ehara, M.; Toyota, K.; Fukuda, R.; Hasegawa, J.; Ishida, M.; Nakajima, T.; Honda, Y.; Kitao, O.; Nakai, H.; Vreven, T.; Montgomery, J. A., Jr.; Peralta, J. E.; Ogliaro, F.; Bearpark, M.; Heyd, J. J.; Brothers, E.; Kudin, K. N.; Staroverov, V. N.; Kobayashi, R.; Normand, J.; Raghavachari, K.; Rendell, A.; Burant, J. C.; Iyengar, S. S.; Tomasi, J.; Cossi, M.; Rega, N.; Millam, J. M.; Klene, M.; Knox, J. E.; Cross, J. B.; Bakken, V.; Adamo, C.; Jaramillo, J.; Gomperts, R.; Stratmann, R. E.; Yazyev, O.; Austin, A. J.; Cammi, R.; Pomelli, C.; Ochterski, J. W.; Martin, R. L.; Morokuma, K.; Zakrzewski, V. G.; Voth, G. A.; Salvador, P.; Dannenberg, J. J.; Dapprich, S.; Daniels, A. D.; Farkas, Ö.; Foresman, J. B.; Ortiz, J. V.; Cioslowski, J.; Fox, D. J. *Gaussian 09*, revision D.01; Gaussian, Inc.: Wallingford, CT, 2010.
(41) Legault, C. Y. *CYLview*, version 1.0b; Universitede Sherbrooke: Quebec, Canada, 2009; http://www.cylview.org.

DOI: 10.1021/acsomega.9b00030
ACS Omega 2019, 4, 5209−5220

(42) (a) Becke, A. D. Density-functional thermochemistry. III. The role of exact exchange. *J. Chem. Phys.* **1993**, *98*, 5648−5652. (b) Lee, C.; Yang, W.; Parr, R. G. Development of the Colle-Salvetti correlation-energy formula into a functional of the electron density. *Phys. Rev. B: Condens. Matter Mater. Phys.* **1988**, *37*, 785−789.
(43) (a) Zhao, Y.; Truhlar, D. G. The M06 Suite of Density Functionals for Main Group Thermochemistry, Thermochemical Kinetics, Noncovalent Interactions, Excited States, and Transition Elements: Two New Functionals and Systematic Testing of Four M06-Class Functionals and 12 Other Functionals. *Theoretical Chemistry Accounts*; Springer, 2008; Vol. *120*, pp 215−241. (b) Zhao, Y.; Truhlar, D. G. Density Functionals with Broad Applicability in Chemistry. *Acc. Chem. Res.* **2008**, *41*, 157−167.
(44) Marenich, A. V.; Cramer, C. J.; Truhlar, D. G. Universal Solvation Model Based on Solute Electron Density and on a Continuum Model of the Solvent Defined by the Bulk Dielectric Constant and Atomic Surface Tensions. *J. Phys. Chem. B* **2009**, *113*, 6378−6396.

DOI: 10.1021/acsomega.9b00030
ACS Omega 2019, 4, 5209−5220